GABAergic Neuroactive Steroids and Resting-State Functional Connectivity in Postpartum Depression: A Preliminary Study

Kristina M. Deligiannidis, M.D.[1,#], **Elif M. Sikoglu, Ph.D.**[2], **Scott A. Shaffer, Ph.D.**[3], **Blaise Frederick, Ph.D.**[4], **Abby Svenson, B.A.**[1], **Andre Kopoyan, B.S.**[3], **Chelsea Kosma, M.A.**[1], **Anthony J. Rothschild, M.D.**[1,*], and **Constance M. Moore, M.Sc., Ph.D.**[2,*]

[1]Center for Psychopharmacologic Research & Treatment, University of Massachusetts Medical School and UMass Memorial Health Care, Worcester, MA, 01605, USA

[2]Center for Comparative Neuroimaging, University of Massachusetts Medical School, Worcester, MA, 01605, USA

[3]Proteomics and Mass Spectrometry Facility, University of Massachusetts Medical School, Worcester, MA 01545, USA

[4]Department of Psychiatry, Harvard Medical School, Boston MA 02115/Brain Imaging Center, McLean Hospital, Belmont MA 02478

Abstract

Postpartum depression (PPD) affects up to 1 in 8 women. The early postpartum period is characterized by a downward physiological shift from relatively elevated levels of sex steroids during pregnancy to diminished levels after parturition. Sex steroids influence functional brain connectivity in healthy non-puerperal subjects. This study tests the hypothesis that PPD is associated with attenuation of resting-state functional connectivity (rs-fc) within corticolimbic regions implicated in depression and alterations in neuroactive steroid concentrations as compared to healthy postpartum women. Subjects (n=32) were prospectively evaluated during pregnancy and in the postpartum with repeated plasma neuroactive steroid measurements and mood and psychosocial assessments. Healthy comparison subjects (HCS) and medication-free subjects with unipolar PPD (PPD) were examined using functional magnetic resonance imaging (fMRI) within 9 weeks of delivery. We performed rs-fc analysis with seeds placed in the anterior cingulate cortex (ACC), and bilateral amygdalae (AMYG), hippocampi (HIPP) and dorsolateral prefrontal cortices (DLPFC). Postpartum rs-fc and perinatal neuroactive steroid plasma concentrations, quantified by liquid chromatography/mass spectrometry, were compared between groups. PPD subjects showed attenuation of connectivity for each of the tested regions (i.e. ACC, AMYG, HIPP and DLPFC) and between corticocortical and corticolimbic regions vs. HCS. Perinatal concentrations of pregnanolone, allopregnanolone and pregnenolone were not different between groups. This is the first report of a disruption in the rs-fc patterns in medication-free subjects with PPD. This disruption may contribute to the development of PPD, at a time of falling neuroactive steroid concentrations.

[#]**Corresponding Author:** Kristina M. Deligiannidis, M.D. Assistant Professor of Psychiatry and Obstetrics & Gynecology Director, Depression Specialty Clinic, University of Massachusetts Medical School, 361 Plantation Street, Worcester, MA 01605, Tel: 508.334.7262, Fax: 508.856.4854, kristina.deligiannidis@umassmemorial.org.
[*]Equal contribution

Keywords

Postpartum depression; functional magnetic resonance imaging; resting-state functional connectivity; neuroactive steroids

INTRODUCTION

Depression is the leading cause of disease burden and years lost to disability for women in their childbearing years (World Health Organization, 2008). Postpartum depression (PPD) affects 1 in 8 women (Cox, JL et al., 1993) and negatively impacts infant attachment, neurocognitive development and behavior (Feldman, R et al., 2009). Women may be at increased risk for developing depression during the postpartum period (Vesga-Lopez, O et al., 2008), a time of a downward physiological shift in sex steroid levels. Current nosology (American Psychiatric Association, 2000) defines PPD as a specifier of a major depressive episode. It is not known if PPD is a distinct neurobiological entity compared to non-puerperal depression (Payne, JL et al., 2009).

Derivatives of progesterone, neuroactive steroids (NAS) alter excitability of the central nervous system through their actions at the γ-aminobutyric acid A (GABA$_A$) receptor (Mostallino, MC et al., 2009; Stell, BM et al., 2003). Times of NAS withdrawal may represent a time of disease vulnerability, as seen in epilepsy (Reddy, DS et al., 2012) and possibly in women predisposed to developing PPD (Bloch, M et al., 2005). Differential regulation of NAS during the perinatal period (Bloch, M et al., 2000; Nappi, RE et al., 2001), may be involved in the pathophysiology of PPD. Alternatively, the GABA$_A$ receptor may undergo NAS induced changes in the perinatal period, acting as a risk factor (Concas, A et al., 1998; Follesa, P et al., 1998; Maguire, J&Mody, I, 2008; 2009).

NAS concentrations are altered in depression (Girdler, SS et al., 2011; Klatzkin, RR et al., 2006) and influence the regulation of emotional responses and affective states in premenstrual syndrome (Schmidt, PJ et al., 1998), and premenstrual dysphoric disorder (PMDD) (Epperson, CN et al., 2002; Girdler, SS et al., 2001). Altered steroid concentrations may reflect abnormalities in the steroid metabolic pathway as elevated ratios of progesterone-derived NAS metabolites to its precursor progesterone have been demonstrated in PMDD and women with a history of depression (Girdler, SS et al., 2011; Girdler, SS et al., 2001; Klatzkin, RR et al., 2006).

Steroids are an important modulator of corticocortical and corticolimbic functional connectivity (Berman, KF et al., 1997; Dreher, JC et al., 2007; Goldstein, JM et al., 2005; van Wingen, GA et al., 2008). Essential to cognitive processing, progesterone and estradiol modulate functional cerebral asymmetries (Weis, S et al., 2008). Progesterone modulates amygdala reactivity (Gingnell, M et al., 2012; Ossewaarde, L et al., 2010; van Wingen, GA et al., 2008) and its connectivity with the prefrontal cortex (Amin, Z et al., 2006; Protopopescu, X et al., 2008). Progesterone, at high levels may reduce amygdala activity (van Wingen, G et al., 2007), but its effects in the postpartum, as levels precipitously decline is unknown.

Although neuroimaging studies in PPD are few, depressive symptomatology in the postpartum period is associated with reduced amygdala responsivity to positive stimuli (Barrett, J et al., 2011), threat-related stimuli (Silverman, ME et al., 2011) and negatively valenced stimuli (Moses-Kolko, EL et al., 2010; Silverman, ME et al., 2007). Additional studies have shown abnormalities in ventral striatal response to reward (Moses-Kolko, EL et al., 2011), increased glutamate levels in the medial prefrontal cortex (McEwen, AM et al.,

2012) and reduced postsynaptic serotonin-1A receptor binding, in particular in the ACC and mesiotemporal cortices (Moses-Kolko, EL et al., 2008). A single study (Epperson, CN et al., 2006) measured NAS. Allopregnanolone and cortical GABA concentrations were low in the postpartum compared to healthy follicular phase women (Epperson, CN et al., 2006).

This investigation is the first to assess resting-state functional connectivity (rs-fc) and quantify NAS concentrations in healthy postpartum subjects and subjects who developed unipolar PPD. Functional connectivity analysis was performed using a hypothesis-driven seed-based approach based on findings in non-puerperal major depression and emerging task-based fMRI and PET findings in PPD described above. We investigated the rs-fc patterns of the anterior cingulate cortex (ACC), amygdala (AMYG), hippocampus (HIPP) and dorsolateral prefrontal cortex (DLPFC). We measured plasma concentrations of two progesterone metabolites, allopregnanolone and pregnanolone and their precursors, progesterone and pregnenolone, to examine if there was an association between perinatal plasma concentrations and PPD or NAS/progesterone ratios and PPD. We tested the hypotheses: (1) PPD would be associated with attenuation of connectivity between the ACC and DLPFC, the ACC and AMYG and the DLPFC and HIPP as compared to healthy postpartum women and (2) mean postpartum plasma concentration of the NAS allopregnanolone (i.e. 3α, 5α-tetrahydroprogesterone) and pregnanolone (i.e. 3α, 5β-tetrahydroprogesterone) would be lower in the PPD group and would be correlated to the postpartum depression total score, and that the ratio of progesterone-derived NAS to progesterone would be elevated in those subjects who developed PPD.

2. MATERIALS AND METHODS

2.1 Subjects

The University of Massachusetts Medical School (UMMS) Institutional Review Board (IRB) granted a waiver to review the medical records of obstetrics patients at UMass Memorial Medical Center during the study period. Subjects who met inclusion/exclusion criteria were approached by study staff to assess interest and eligibility. Two-hundred and forty-three subjects were consented and screened with the Edinburgh Postnatal Depression Scale (EPDS) (Cox, JL et al., 1987) at 26–30 weeks gestational age. The EPDS is a well-validated self-report of depression and anxiety symptoms used to assess perinatal depression (Bergink, V et al., 2011; Cox, JL et al., 1987). A total of 32 eligible subjects of 18–40 years of age enrolled in the prospective study. Sample size was limited by available funding for this preliminary study. Two groups were enrolled: (1) 12 healthy control subjects (HCS) who were at low-risk and (2) 20 subjects at high-risk for developing postpartum depression (PPD). The HCS group included women without a personal or family history of psychiatric illness, as ascertained by clinical and research interviews [(Mini International Neuropsychiatric Interview (MINI) (Sheehan, DV et al., 1998) conducted by a board-certified psychiatrist (K.M.D.)] and who had an EPDS 5 throughout pregnancy and the postpartum, which indicated the absence of depressive or anxiety symptoms. At the time of the postpartum MRI scan, HCS continued to have no psychiatric symptoms. Since women with anxiety or depressive symptoms during pregnancy, or a history of PPD are at increased risk of future PPD episodes, (Viguera, AC et al., 2011), the PPD subject group included subjects who had a history of major depressive disorder (MDD) or PPD and an EPDS 10 at the first study visit (i.e. at 26–30 weeks gestation). The EPDS cut-off of 10 was chosen based on validation of the EPDS during pregnancy (Bergink, V et al., 2011). Subjects who had a score of 6–9 on the EPDS or had an EPDS 10 and met criteria for major depression at the time of screening were ineligible. All 32 subjects completed all four study visits. In the HCS group, 9/12 subjects consented to the MRI scan. In the high risk (PPD) group 12/20 subjects developed PPD. Of those 12 subjects, 8 subjects consented to the MRI scan. All

data reported represents 9 HCS and 8 high-risk subjects who developed PPD and completed resting-state functional Magnetic Resonance Imaging (rs-fMRI).

Subjects were excluded if they had: a multiple gestation pregnancy, a current major depressive episode or lifetime history of manic episode or any psychotic disorder as determined by the MINI; elevated suicidal risk; alcohol, tobacco or substance abuse/ dependence in the 6 months prior to study entry; positive urine benzodiazepine test; positive urine pregnancy test prior to MRI; pregnancy loss; active or history of serious medical, neurological or endocrine disorder; any contraindication to MRI; antidepressant or benzodiazepine use 4 weeks prior to study entry and at any time during the study; concomitant use of pharmacotherapy with known psychotropic, GABAergic or neurosteroidotropic activity at any time during the study.

2.2 Procedures

All subjects were evaluated during pregnancy (i.e. between 26–30 weeks gestation (visit 1) and 34–36 weeks gestation (visit 2), dates confirmed by first trimester ultrasound) and in the postpartum (i.e. <36 hours after parturition (visit 3) and between 3–9 weeks after parturition (visit 4)). The 9-week postpartum cut-off was based on literature suggesting a postpartum onset definition of up to 6–8 weeks of delivery as optimal(Forty, L et al., 2006), with the additional week to allow research assessment completion. Serial mood and psychosocial assessments were completed at each of the four study visits. Blood samples for NAS analysis were obtained at antepartum study visit 2 and postpartum study visit 4 between 9– 11 AM, whenever possible, and collected into tubes containing EDTA. Samples were centrifuged at 4,000 rpm for 15 minutes and plasma was stored at −80°C until analysis was completed by collaborators blind to the mood outcome. Research assessments done at all 4 visits included: Edinburgh Postnatal Depression Scale (EPDS) (Cox, JL et al., 1987), Quick Inventory of Depressive Symptoms –self report (QIDS-SR) (Rush, AJ et al., 2003), Sheehan Patient Rated Anxiety Scale (SPRAS) (Sheehan, DV, 1983), Pittsburgh Sleep Quality Index (PSQI) (Buysse, DJ et al., 1989), Sheehan Disability Scale (SDS) (Sheehan, DV, 1983) and urine benzodiazepine test. Assessments done at visit 1 included the MINI and past medical history/demographics. Additional assessments done at the final study visit (visit 4) included (Table 1): MINI, Postpartum Social Support Questionnaire (PSSQ) (Hopkins, J&Campbell, SB, 2008), Mother-to-Infant Bonding Scale (MIBS) (Taylor, A et al., 2005), Labor and Delivery Questionnaire, Menses & breastfeeding recording, urine pregnancy test and rs- fMRI.

All subjects who underwent rs-fMRI delivered a healthy, term infant and were medication- free and breastfeeding and/or bottle-feeding. An MRI was not performed for subjects in the high-risk group who did not develop PPD or any subject who later did not consent to the postpartum MRI. Study data was managed using Research Electronic Data Capture (REDCap) (Harris, PA et al., 2009). Subjects provided written informed consent as approved by the UMMS IRB and each received monetary compensation.

2.3 Resting-state functional connectivity

2.3a Image acquisition—Data were acquired on a 3.0 Tesla Philips Achieva whole-body MR system (Philips Healthcare, Best, the Netherlands) with an 8 element phased-array head coil at the Advanced MRI Center, UMMS. T1-weighted anatomical MRI (MPRAGE sequence, 256×252 voxels, TR: 6.76 msec, TE: 3.1 msec, FOV: 244 mm × 256 mm × 204 mm, 170 slices, 560 sec) were collected for diagnostic and localization purposes. All of the subjects underwent the resting-state fMRI scan with open eyes (Friston, KJ, 1994) and were instructed to attend to a static frame projected onto the screen which was visible through a mirror mounted on the head coil. The static frame contained a white plus-sign superimposed

on the middle of a black background. Resting-state scan images were obtained using an EPI sequence (84×81 voxels, FOV: 256mm × 256mm, TR: 2500 msec, TE: 30 msec, flip angle: 75°, slice thickness: 3 mm, 50 slices). Diagnostic scans were evaluated by a neuroradiologist: no abnormalities were identified.

2.3b Data analysis—Resting-state fMRI data analysis was carried out by using Data Processing Assistant for Resting-State fMRI (DPARSFA-http://www.restfmri.net) (Song, XW et al., 2011). DPARFSA is plug-in software that works with SPM8 (Statistical Parameter Mapping– Welcome Department of Imaging Neuroscience, London, UK; (http://www.fil.ion.ucl.ac.uk/spm/software/spm8/) and the Resting-State fMRI Data Analysis toolkit (REST). The visualization was done using xjView toolkit (http://www.alivelearn.net/xjview8/). Images were corrected for slice acquisition time differences, realigned, normalized, spatially smoothed with a 4 mm FWHM kernel, detrended and temporally band-pass filtered to 0.01–0.08 Hz (Chai, XJ et al., 2011a). An independent component-based noise correction method was used to regress-out physiological and other sources of noise such as white matter and cerebrospinal fluid signals and head motion related covariates. Functional connectivity analysis was performed using a hypothesis-driven seed-based approach; the connectivity patterns from ACC, left and right AMYG, left and right HIPP, left and right DLPFC were investigated (Table 2). First-level analysis consisted of extracting the average blood-oxygenation level dependent (BOLD) time courses from each seed and computing the Pearson's correlation coefficients between this average time course and the BOLD time course of every other voxel. These correlation coefficients were then converted to normally distributed z-scores using Fisher's z-transform. First-level analysis was performed for each subject. Through the second-level analysis, group functional connectivity maps with each seed were formed using 1-sample t-test for subjects with PPD and HCS. The two groups' resting-state functional connections with each seed were compared voxelwise using a 2-sample t-test. The resulting maps were thresholded using $p<0.01$ family-wise error correction for multiple comparisons with an extent of more than 5 contiguous voxels and subjected to cluster analysis.

2.4 Neuroactive steroid quantification

2.4a Materials—Progesterone (CAS 57-83-0) and pregnenolone (CAS 145-13-1) were purchased from Steraloids, Inc. (Newport, RI). Allopregnanolone (CAS 516-54-1), pregnanolone (CAS 128-20-1), d_4-pregnenolone, and d_9-progesterone were synthesized by Dr. Robert H. Purdy (Veterans Medical Research Foundation, San Diego, CA). Labeled d_4-allopregnanolone and d_4-pregnanolone were obtained through CDN Isotopes, Inc. (Pointe-Claire, Canada). Human male charcoal-stripped plasma was purchased from Bioreclamation, LLC (Westbury, NY).

2.4b Extraction and Calibration—NAS were extracted from plasma using a two-step solid-phase extraction (SPE) procedure. In brief, plasma aliquots (300 μL) were spiked with a mixture containing 7.75 ng each of d_4-pregnenolone, d_9-progesterone, d_4-allopregnanolone and d_4-pregnanolone. Samples were applied to a 500 mg C18 SPE cartridge (Agilent Technologies, Santa Clara, CA) preconditioned with methanol followed by water. After washing with water followed by 40% methanol, NAS were eluted with 2.5 mL of methanol. Eluates were then dried, re-suspended in 2 mL of ethyl acetate/methanol (4:1), and then applied to a 500 mg aminopropyl SPE cartridge (Agilent) preconditioned with ethyl acetate followed by ethyl acetate/methanol (80:20). NAS were eluted with 2.5 mL ethyl acetate/methanol (4:1), dried, and re-suspended for LC-MS/MS analysis in 20 μL of 40% methanol containing 0.1% (v/v) formic acid and 2mM lithium acetate.

Samples were measured against a 7-point calibration curve (0.2, 0.5, 5.0, 25.0, 50.0, 500, 1000 ng/mL) of NAS prepared from human, male charcoal-stripped plasma. Stocks solutions of NAS were prepared and spiked at each of the standard concentrations as a 10 μL aliquot into 290 μL charcoal-stripped plasma. In addition, each calibration point was spiked with the internal standard mixture as described above. Blank plasma was also prepared both with and without internal standard. The standard curve was prepared in duplicate and extracted according to same method as described for the samples.

2.4c LC-MS/MS Analysis—NAS were analyzed on a NanoAcquity UPLC (Waters Corporation, Milford, MA) coupled to a Quattro Premier XE (*Waters*) triple quadrupole mass spectrometer operating in the positive ion electrospray mode. In brief, calibrants and samples were loaded in 40% methanol (containing 0.1% formic acid and 2mM lithium acetate) onto a custom-made trap column (180 μm I.D. fused silica with Kasil frit) containing 1.5 cm of 3 μm (100Å) Magic C18AQ particles (Michrom Bioresources, Auburn, CA). NAS were then eluted at 1.5 μL/min using a custom-made analytical column (150 μm I.D. fused silica) with a gravity-pulled tip and packed with 20 cm of 3 μm (100Å) Magic C18AQ particles. Initial conditions were 40% methanol (containing 0.1% formic acid and 2mM lithium acetate) for one minute followed by a fast linear gradient to 90% methanol (containing 0.1% formic acid and 2mM lithium acetate) from 1–2 minutes and held until 15.5 minutes before returning to initial conditions. Data were acquired using multiple reaction monitoring (MRM) using the precursor to fragment transition corresponding to $(M + Li + H_2O)^+ > (M + Li)^+$. Samples and calibrants were injected in duplicate and quantified using QuanLynx (Version 4.1, *Waters*) using a linear fit (origin excluded) with a 1/x axis weighting.

2.5 Statistical analysis

Fisher's exact test for categorical and Mann-Whitney U tests for continuous variables were carried out (Table 1) using SPSS 19 to examine differences in demographic, medical and psychiatric history and current diagnostic and psychosocial measures between PPD and HCS subjects.

Mann-Whitney U tests for continuous variables were carried out (Table 3) using SPSS 19 to compare the differences in progesterone, pregnenolone, pregnanolone and allopregnanolone concentrations between groups. Differences in steroid concentrations (Table 3) and ratios of allopregnanolone/progesterone, pregnanolone/progesterone, pregnenolone/progesterone, [allopregnanolone + pregnenolone]/progesterone and [allopregnanolone + pregnanolone]/ progesterone were compared between groups at the 34–36 week pregnancy and postpartum MRI time points.

Pearson correlation analyses were carried out to investigate the relationship between antepartum and postpartum steroid concentrations and NAS/progesterone ratios and postpartum EPDS total score at time of MRI using data pooled from both groups due to small subject numbers. The relationship between postpartum steroid concentrations and NAS/progesterone ratios and the number of days since parturition was examined to determine if groups were similarly matched in regards to the expected physiological postpartum rise in progesterone which follows the immediate fall at parturition.

3. RESULTS

3.1 Demographic factors

As summarized in Table 1, there were no significant differences between HCS and PPD in age, right-handedness, delivery type, breastfeeding status, presence of any menstrual

spotting, or time since delivery relative to the day of MRI. Women who entered the study in the high risk group and developed PPD had a history of major depression (p<0.001), and generalized anxiety (p<0.05), at rates significantly higher than the low risk, healthy group, who had none. 25% of women who developed PPD had a history of prior PPD (p=ns). Women with PPD had greater symptomatology than the HCS group as measured by significantly higher EPDS, QIDS, SPRAS and SDS scores.

3.2 Resting-state functional connectivity

Corticocortical and corticolimbic connectivity was significantly stronger in HCS relative to subjects with PPD between numerous pairs of regions as shown in Table 2. The HCS group had significantly stronger connectivity between the ACC and left DLPFC and bilateral AMYG; between bilateral AMYG and ACC and bilateral DLPFC; between the left DLPFC and right AMYG, right HIPP and right DLPFC than the PPD group.

3.3 Neuroactive steroid concentrations and ratios during pregnancy and at the time of postpartum MRI scan

Table 3 summarizes concentrations (ng/mL) of progesterone, pregnenolone, pregnanolone and allopregnanolone as quantified by LC/MS. Progesterone concentration had a significant positive relationship to the number of days since delivery: r=0.74, p=0.004 but there was no difference between-groups (p>0.05). NAS concentrations between groups did not significantly differ during pregnancy or the postpartum (p>0.05). The relationship between the concentration of allopregnanolone during pregnancy and the postpartum EPDS total score at the time of MRI did not reach significance(r=0.696, p=0.083).

NAS/progesterone ratios at the time of postpartum MRI had a negative relationship with the number of days since delivery but there was no difference between-groups: allopregnanolone/progesterone (r=−0.89, p<0.001); pregnenolone/progesterone (r=−0.92, p<0.001); pregnanolone/progesterone (r=−0.76, p<0.004); [allopregnanolone + pregnenolone]/ progesterone (r=−0.91, p<0.001) and [allopregnanolone + pregnanolone]/ progesterone (r=−0.81, p<0.001). NAS ratios in pregnancy or at the time of postpartum MRI did not significantly differ between groups (p>0.05).

4. DISCUSSION

The present investigation is the first to report altered resting-state functional connectivity in corticocortical and corticolimbic functional connections in PPD vs. healthy postpartum subjects. The HCS group had significantly stronger connectivity between the ACC and left DLPFC and bilateral AMYG; between bilateral AMYG and ACC and bilateral DLPFC; between the left DLPFC and right AMYG, right HIPP and right DLPFC than the PPD group. Our preliminary results demonstrate similarity between rs-fc findings in non-puerperal and puerperal MDD. Non-puerperal depression is hypothesized to be a consequence of dysregulation in corticolimbic pathways (Fitzgerald, PB et al., 2008; Mayberg, HS, 2003). In non-puerperal MDD, reduced connectivity exists between cortical, including the dorsal anterior cingulate cortex (dACC), and limbic regions (Anand, A et al., 2005; Greicius, MD et al., 2007). Decreases in orbitofrontal cortex-precuneus connectivity (Frodl, T et al., 2009), pregenual anterior cingulate cortex-dorsomedial thalamus connectivity (Anand, A et al., 2009) and bilateral AMYG connectivity(Veer, IM et al., 2009) and increased subgenual cingulate-thalamic connectivity(Greicius, MD et al., 2007) have been reported in non-puerperal major depression. Functional MRI studies have shown hypoactivation of the stress response circuitry [hypothalamus, AMYG, HIPP, ACC, and orbitofrontal cortex] in women with remitted MDD (Holsen, LM et al., 2011): in this study,

subjects with a current depressive episode had attenuated rs-fc in some of those same regions, i.e. the AMYG, HIPP and ACC.

It is not known if puerperal and non-puerperal MDD share a unifying etiology or if perinatal NAS impact neural circuitry, influencing the expression of the disorder during the postpartum downward shift in sex steroids. In this study, NAS concentrations and NAS/progesterone ratios in pregnancy or at the time of postpartum MRI did not significantly differ between groups. It is possible that peripheral steroid concentrations may not directly reflect central nervous system concentrations or the absolute plasma steroid concentration may not be a central factor for the development of either PPD or observed differences in connectivity observed between groups. Because of our limited sample size, we cannot rule out the existence of true differences between groups, however this potential marker of risk warrants further investigation.

Despite the importance of understanding how NAS modulate functional connectivity at times of fluctuating levels of sex steroids, there are several limitations to this preliminary study. In a small sample, we report robust between-group differences in connectivity with the ACC, AMYG, HIPP and DLPFC and other regions of interest. Replication of these results and investigation of additional brain regions, e.g. thalamus, orbitofrontal cortex is needed. This study matched subjects on time from delivery, however the changes in maternal perinatal physiology might cause fluctuations in hemodynamic response in the brain, which may be associated with the differences in BOLD signal as well as blood or respiratory volume and cardiac input/output (Bandettini, PA, 2009). In order to eliminate the possible effect of cerebral metabolic changes, a multimodal study including positron emission tomography (PET) might be considered.

Another limitation to this study was that it was possible that subjects were at different stages in resumption of ovulation based on time from delivery and breastfeeding status, two variables upon which we matched subjects. However, as expected, progesterone concentration was positively correlated to the number of days since parturition while NAS/progesterone ratios at the time of postpartum MRI had a negative relationship with the number of days since parturition, reflecting rising progesterone and falling NAS concentrations in the postpartum. There were no between-group differences on these measures at the time of MRI, suggesting that the groups were similarly matched. 87.5% of the PPD group had a history of major depression, so it is not certain if the observed differences in rs-fc reflect state vs. trait differences, a limitation of many studies (Hasler, G&Northoff, G, 2011). Due to the preliminary nature of this study, we did not exclude subjects who had a prior history of non-puerperal MDD; however the study design would have been stronger if only subjects with a history of PPD were included so that the studied neurobiological differences would be associated with a more stringent phenotype. Additionally, many subjects in the PPD group had a comorbid anxiety disorder compared to the HCS. The presence of comorbid anxiety disorder makes the delineation of shared functional circuits challenging to parse out, but accurately reflects the clinical symptomatology of women with PPD.

Strengths of the study include its longitudinal design which allowed repeated evaluation of mood, anxiety, sleep and disability throughout the perinatal period and allowed MRI to be used immediately after subjects developed PPD but before they initiated pharmacotherapy or hormonal contraception. Depressed women who completed the MRI had symptoms of moderate severity. Four women who developed severe PPD declined the MRI scan due to the severity of depressive and anxiety symptomatology. Research on a larger or more severely ill group may reveal further differences in connectivity or significant differences in steroid concentrations and measures of postpartum support and mother-infant bonding.

The present investigation is the first to report attenuation of corticocortical and corticolimbic resting-state functional connectivity and to prospectively quantify NAS concentrations in women who developed unipolar PPD as compared to healthy postpartum women. Future studies will benefit from including a group with non-puerperal depression and a larger sample size to fully power correlation analyses of rs-fc and steroid concentrations as well as include demographic and clinical measures as covariates into the rs-fc analysis. It would be beneficial to acquire antepartum resting-state fMRI data to assess the changes in functional connectivity on subject-by-subject basis. These next-step studies will increase our understanding of the pathophysiology of depression which occurs during a time of falling sex steroid levels.

REFERENCES

World Health Organization. Switzerland: Department of Health Statistics and Informatics; Information, Evidence and Research Cluster of the World Health Organization; 2008. The Global Burden of Disease: 2004 update; p. 36-49.

American Psychiatric Association. Diagnostic and Statistical Manual of Mental Disorders. Washington, DC: American Psychiatric Association; 2000.

Amin Z, Epperson CN, Constable RT, Canli T. Effects of estrogen variation on neural correlates of emotional response inhibition. Neuroimage. 2006; 32:457–464. [PubMed: 16644236]

Anand A, Li Y, Wang Y, Lowe MJ, Dzemidzic M. Resting state corticolimbic connectivity abnormalities in unmedicated bipolar disorder and unipolar depression. Psychiatry Res. 2009; 171:189–198. [PubMed: 19230623]

Anand A, Li Y, Wang Y, Wu J, Gao S, Bukhari L, Mathews VP, Kalnin A, Lowe MJ. Activity and connectivity of brain mood regulating circuit in depression: a functional magnetic resonance study. Biol Psychiatry. 2005; 57:1079–1088. [PubMed: 15866546]

Bandettini PA. What's new in neuroimaging methods? Ann N Y Acad Sci. 2009; 1156:260–293. [PubMed: 19338512]

Barrett J, Wonch KE, Gonzalez A, Ali N, Steiner M, Hall GB, Fleming AS. Maternal affect and quality of parenting experiences are related to amygdala response to infant faces. Soc Neurosci. 2011

Bergink V, Kooistra L, Lambregtse-van den Berg MP, Wijnen H, Bunevicius R, van Baar A, Pop V. Validation of the Edinburgh Depression Scale during pregnancy. J Psychosom Res. 2011; 70:385–389. [PubMed: 21414460]

Berman KF, Schmidt PJ, Rubinow DR, Danaceau MA, Van Horn JD, Esposito G, Ostrem JL, Weinberger DR. Modulation of cognition-specific cortical activity by gonadal steroids: a positron-emission tomography study in women. Proc Natl Acad Sci U S A. 1997; 94:8836–8841. [PubMed: 9238064]

Blakemore SJ. The social brain in adolescence. Nature reviews Neuroscience. 2008; 9:267–277.

Bloch M, Rubinow DR, Schmidt PJ, Lotsikas A, Chrousos GP, Cizza G. Cortisol response to ovine corticotropin-releasing hormone in a model of pregnancy and parturition in euthymic women with and without a history of postpartum depression. J Clin Endocrinol Metab. 2005; 90:695–699. [PubMed: 15546899]

Bloch M, Schmidt PJ, Danaceau M, Murphy J, Nieman L, Rubinow DR. Effects of gonadal steroids in women with a history of postpartum depression. Am J Psychiatry. 2000; 157:924–930. [PubMed: 10831472]

Buysse DJ, Reynolds CF 3rd, Monk TH, Berman SR, Kupfer DJ. The Pittsburgh Sleep Quality Index: a new instrument for psychiatric practice and research. Psychiatry Res. 1989; 28:193–213. [PubMed: 2748771]

Chai XJ, Whitfield-Gabrieli S, Shinn AK, Gabrieli JD, Nieto Castanon A, McCarthy JM, Cohen BM, Ongur D. Abnormal medial prefrontal cortex resting-state connectivity in bipolar disorder and schizophrenia. Neuropsychopharmacology. 2011a; 36:2009–2017. [PubMed: 21654735]

Chai XJ, Whitfield-Gabrieli S, Shinn AK, Gabrieli JD, Nieto Castanon A, McCarthy JM, Cohen BM, Ongur D. Abnormal medial prefrontal cortex resting-state connectivity in bipolar disorder and schizophrenia. Neuropsychopharmacology. 2011b; 36:2009–2017. [PubMed: 21654735]

Concas A, Mostallino MC, Porcu P, Follesa P, Barbaccia ML, Trabucchi M, Purdy RH, Grisenti P, Biggio G. Role of brain allopregnanolone in the plasticity of gamma-aminobutyric acid type A receptor in rat brain during pregnancy and after delivery. Proc Natl Acad Sci U S A. 1998; 95:13284–13289. [PubMed: 9789080]

Conklin SM, Gianaros PJ, Brown SM, Yao JK, Hariri AR, Manuck SB, Muldoon MF. Long-chain omega-3 fatty acid intake is associated positively with corticolimbic gray matter volume in healthy adults. Neurosci Lett. 2007; 421:209–212. [PubMed: 17574755]

Cox JL, Holden JM, Sagovsky R. Detection of postnatal depression. Development of the 10-item Edinburgh Postnatal Depression Scale. Br J Psychiatry. 1987; 150:782–786. [PubMed: 3651732]

Cox JL, Murray D, Chapman G. A controlled study of the onset, duration and prevalence of postnatal depression. Br J Psychiatry. 1993; 163:27–31. [PubMed: 8353695]

Cullen KR, Gee DG, Klimes-Dougan B, Gabbay V, Hulvershorn L, Mueller BA, Camchong J, Bell CJ, Houri A, Kumra S, Lim KO, Castellanos FX, Milham MP. A preliminary study of functional connectivity in comorbid adolescent depression. Neuroscience letters. 2009; 460:227–231. [PubMed: 19446602]

Dreher JC, Schmidt PJ, Kohn P, Furman D, Rubinow D, Berman KF. Menstrual cycle phase modulates reward-related neural function in women. Proc Natl Acad Sci U S A. 2007; 104:2465–2470. [PubMed: 17267613]

Epperson CN, Gueorguieva R, Czarkowski KA, Stiklus S, Sellers E, Krystal JH, Rothman DL, Mason GF. Preliminary evidence of reduced occipital GABA concentrations in puerperal women: a 1H-MRS study. Psychopharmacology (Berl). 2006; 186:425–433. [PubMed: 16724188]

Epperson CN, Haga K, Mason GF, Sellers E, Gueorguieva R, Zhang W, Weiss E, Rothman DL, Krystal JH. Cortical gamma-aminobutyric acid levels across the menstrual cycle in healthy women and those with premenstrual dysphoric disorder: a proton magnetic resonance spectroscopy study. Arch Gen Psychiatry. 2002; 59:851–858. [PubMed: 12215085]

Ernst M, Nelson EE, Jazbec S, McClure EB, Monk CS, Leibenluft E, Blair J, Pine DS. Amygdala and nucleus accumbens in responses to receipt and omission of gains in adults and adolescents. Neuroimage. 2005; 25:1279–1291. [PubMed: 15850746]

Evans KC, Wright CI, Wedig MM, Gold AL, Pollack MH, Rauch SL. A functional MRI study of amygdala responses to angry schematic faces in social anxiety disorder. Depress Anxiety. 2008; 25:496–505. [PubMed: 17595018]

Feldman R, Granat A, Pariente C, Kanety H, Kuint J, Gilboa-Schechtman E. Maternal depression and anxiety across the postpartum year and infant social engagement, fear regulation, and stress reactivity. J Am Acad Child Adolesc Psychiatry. 2009; 48:919–927. [PubMed: 19625979]

Fitzgerald PB, Laird AR, Maller J, Daskalakis ZJ. A meta-analytic study of changes in brain activation in depression. Hum Brain Mapp. 2008; 29:683–695. [PubMed: 17598168]

Follesa P, Floris S, Tuligi G, Mostallino MC, Concas A, Biggio G. Molecular and functional adaptation of the GABA(A) receptor complex during pregnancy and after delivery in the rat brain. Eur J Neurosci. 1998; 10:2905–2912. [PubMed: 9758160]

Forty L, Jones L, Macgregor S, Caesar S, Cooper C, Hough A, Dean L, Dave S, Farmer A, McGuffin P, Brewster S, Craddock N, Jones I. Familiality of postpartum depression in unipolar disorder: results of a family study. Am J Psychiatry. 2006; 163:1549–1553. [PubMed: 16946179]

Friston KJ. Functional and effective connectivity in neuroImaging: A synthesis. Human Brain Mapping. 1994; 2:56–78.

Frodl T, Scheuerecker J, Albrecht J, Kleemann AM, Muller-Schunk S, Koutsouleris N, Moller HJ, Bruckmann H, Wiesmann M, Meisenzahl E. Neuronal correlates of emotional processing in patients with major depression. World J Biol Psychiatry. 2009; 10:202–208. [PubMed: 17965984]

Gianaros PJ, Sheu LK, Matthews KA, Jennings JR, Manuck SB, Hariri AR. Individual differences in stressor-evoked blood pressure reactivity vary with activation, volume, and functional connectivity of the amygdala. J Neurosci. 2008; 28:990–999. [PubMed: 18216206]

Gingnell M, Morell A, Bannbers E, Wikstrom J, Sundstrom Poromaa I. Menstrual cycle effects on amygdala reactivity to emotional stimulation in premenstrual dysphoric disorder. Horm Behav. 2012; 62:400–406. [PubMed: 22814368]

Girdler SS, Lindgren M, Porcu P, Rubinow DR, Johnson JL, Morrow AL. A history of depression in women is associated with an altered GABAergic neuroactive steroid profile. Psychoneuroendocrinology. 2011

Girdler SS, Straneva PA, Light KC, Pedersen CA, Morrow AL. Allopregnanolone levels and reactivity to mental stress in premenstrual dysphoric disorder. Biol Psychiatry. 2001; 49:788–797. [PubMed: 11331087]

Goldstein JM, Jerram M, Poldrack R, Ahern T, Kennedy DN, Seidman LJ, Makris N. Hormonal cycle modulates arousal circuitry in women using functional magnetic resonance imaging. J Neurosci. 2005; 25:9309–9316. [PubMed: 16207891]

Greicius MD, Flores BH, Menon V, Glover GH, Solvason HB, Kenna H, Reiss AL, Schatzberg AF. Resting-state functional connectivity in major depression: abnormally increased contributions from subgenual cingulate cortex and thalamus. Biol Psychiatry. 2007; 62:429–437. [PubMed: 17210143]

Harris PA, Taylor R, Thielke R, Payne J, Gonzalez N, Conde JG. Research electronic data capture (REDCap)--a metadata-driven methodology and workflow process for providing translational research informatics support. J Biomed Inform. 2009; 42:377–381. [PubMed: 18929686]

Hasler G, Northoff G. Discovering imaging endophenotypes for major depression. Mol Psychiatry. 2011; 16:604–619. [PubMed: 21602829]

Hayama HR, Rugg MD. Right dorsolateral prefrontal cortex is engaged during post-retrieval processing of both episodic and semantic information. Neuropsychologia. 2009; 47:2409–2416. [PubMed: 19383503]

Holsen LM, Spaeth SB, Lee JH, Ogden LA, Klibanski A, Whitfield-Gabrieli S, Goldstein JM. Stress response circuitry hypoactivation related to hormonal dysfunction in women with major depression. J Affect Disord. 2011; 131:379–387. [PubMed: 21183223]

Hopkins J, Campbell SB. Development and validation of a scale to assess social support in the postpartum period. Arch Womens Ment Health. 2008; 11:57–65. [PubMed: 18317709]

Kahn I, Andrews-Hanna JR, Vincent JL, Snyder AZ, Buckner RL. Distinct cortical anatomy linked to subregions of the medial temporal lobe revealed by intrinsic functional connectivity. J Neurophysiol. 2008; 100:129–139. [PubMed: 18385483]

Kelly AM, Di Martino A, Uddin LQ, Shehzad Z, Gee DG, Reiss PT, Margulies DS, Castellanos FX, Milham MP. Development of anterior cingulate functional connectivity from late childhood to early adulthood. Cerebral cortex. 2009; 19:640–657. [PubMed: 18653667]

Klatzkin RR, Morrow AL, Light KC, Pedersen CA, Girdler SS. Associations of histories of depression and PMDD diagnosis with allopregnanolone concentrations following the oral administration of micronized progesterone. Psychoneuroendocrinology. 2006; 31:1208–1219. [PubMed: 17046166]

Maguire J, Mody I. GABA(A)R plasticity during pregnancy: relevance to postpartum depression. Neuron. 2008; 59:207–213. [PubMed: 18667149]

Maguire J, Mody I. Steroid hormone fluctuations and GABA(A)R plasticity. Psychoneuroendocrinology. 2009; 34(Suppl 1):S84–S90. [PubMed: 19632051]

Margulies DS, Kelly AM, Uddin LQ, Biswal BB, Castellanos FX, Milham MP. Mapping the functional connectivity of anterior cingulate cortex. NeuroImage. 2007; 37:579–588. [PubMed: 17604651]

Mayberg HS. Modulating dysfunctional limbic-cortical circuits in depression: towards development of brain-based algorithms for diagnosis and optimised treatment. Br Med Bull. 2003; 65:193–207. [PubMed: 12697626]

McClure SM, Li J, Tomlin D, Cypert KS, Montague LM, Montague PR. Neural correlates of behavioral preference for culturally familiar drinks. Neuron. 2004; 44:379–387. [PubMed: 15473974]

McEwen AM, Burgess DT, Hanstock CC, Seres P, Khalili P, Newman SC, Baker GB, Mitchell ND, Khudabux-Der J, Allen PS, Lemelledo JM. Increased Glutamate Levels in the Medial Prefrontal Cortex in Patients with Postpartum Depression. Neuropsychopharmacology. 2012

Moses-Kolko EL, Fraser D, Wisner KL, James JA, Saul AT, Fiez JA, Phillips ML. Rapid habituation of ventral striatal response to reward receipt in postpartum depression. Biol Psychiatry. 2011; 70:395–399. [PubMed: 21507385]

Moses-Kolko EL, Perlman SB, Wisner KL, James J, Saul AT, Phillips ML. Abnormally reduced dorsomedial prefrontal cortical activity and effective connectivity with amygdala in response to negative emotional faces in postpartum depression. Am J Psychiatry. 2010; 167:1373–1380. [PubMed: 20843875]

Moses-Kolko EL, Wisner KL, Price JC, Berga SL, Drevets WC, Hanusa BH, Loucks TL, Meltzer CC. Serotonin 1A receptor reductions in postpartum depression: a positron emission tomography study. Fertil Steril. 2008; 89:685–692. [PubMed: 17543959]

Mostallino MC, Sanna E, Concas A, Biggio G, Follesa P. Plasticity and function of extrasynaptic GABA(A) receptors during pregnancy and after delivery. Psychoneuroendocrinology. 2009

Nappi RE, Petraglia F, Luisi S, Polatti F, Farina C, Genazzani AR. Serum allopregnanolone in women with postpartum "blues". Obstet Gynecol. 2001; 97:77–80. [PubMed: 11152912]

Ossewaarde L, Hermans EJ, van Wingen GA, Kooijman SC, Johansson IM, Backstrom T, Fernandez G. Neural mechanisms underlying changes in stress-sensitivity across the menstrual cycle. Psychoneuroendocrinology. 2010; 35:47–55. [PubMed: 19758762]

Payne JL, Palmer JT, Joffe H. A reproductive subtype of depression: conceptualizing models and moving toward etiology. Harv Rev Psychiatry. 2009; 17:72–86. [PubMed: 19373617]

Protopopescu X, Tuescher O, Pan H, Epstein J, Root J, Chang L, Altemus M, Polanecsky M, McEwen B, Stern E, Silbersweig D. Toward a functional neuroanatomy of premenstrual dysphoric disorder. J Affect Disord. 2008; 108:87–94. [PubMed: 18031826]

Qin S, Hermans EJ, van Marle HJ, Luo J, Fernandez G. Acute psychological stress reduces working memory-related activity in the dorsolateral prefrontal cortex. Biol Psychiatry. 2009; 66:25–32. [PubMed: 19403118]

Reddy DS, Gould J, Gangisetty O. A Mouse Kindling Model of Perimenstrual Catamenial Epilepsy. J Pharmacol Exp Ther. 2012

Rush AJ, Trivedi MH, Ibrahim HM, Carmody TJ, Arnow B, Klein DN, Markowitz JC, Ninan PT, Kornstein S, Manber R, Thase ME, Kocsis JH, Keller MB. The 16-Item Quick Inventory of Depressive Symptomatology (QIDS), clinician rating (QIDS-C), and self-report (QIDS-SR): a psychometric evaluation in patients with chronic major depression. Biol Psychiatry. 2003; 54:573–583. [PubMed: 12946886]

Schmidt PJ, Nieman LK, Danaceau MA, Adams LF, Rubinow DR. Differential behavioral effects of gonadal steroids in women with and in those without premenstrual syndrome. N Engl J Med. 1998; 338:209–216. [PubMed: 9435325]

Sheehan, DV. The Anxiety Disease. New York: Charles Scribner & Sons; 1983.

Sheehan DV, Lecrubier Y, Sheehan KH, Amorim P, Janavs J, Weiller E, Hergueta T, Baker R, Dunbar GC. The Mini-International Neuropsychiatric Interview (M.I.N.I.): the development and validation of a structured diagnostic psychiatric interview for DSM-IV and ICD-10. J Clin Psychiatry. 1998; 59(Suppl 20):22–33. quiz 34–57. [PubMed: 9881538]

Shin LM, Wright CI, Cannistraro PA, Wedig MM, McMullin K, Martis B, Macklin ML, Lasko NB, Cavanagh SR, Krangel TS, Orr SP, Pitman RK, Whalen PJ, Rauch SL. A functional magnetic resonance imaging study of amygdala and medial prefrontal cortex responses to overtly presented fearful faces in posttraumatic stress disorder. Arch Gen Psychiatry. 2005; 62:273–281. [PubMed: 15753240]

Silton RL, Heller W, Towers DN, Engels AS, Spielberg JM, Edgar JC, Sass SM, Stewart JL, Sutton BP, Banich MT, Miller GA. The time course of activity in dorsolateral prefrontal cortex and anterior cingulate cortex during top-down attentional control. Neuroimage. 2010; 50:1292–1302. [PubMed: 20035885]

Silverman ME, Loudon H, Liu X, Mauro C, Leiter G, Goldstein MA. The neural processing of negative emotion postpartum: a preliminary study of amygdala function in postpartum depression. Arch Womens Ment Health. 2011; 14:355–359. [PubMed: 21713456]

Silverman ME, Loudon H, Safier M, Protopopescu X, Leiter G, Liu X, Goldstein M. Neural dysfunction in postpartum depression: an fMRI pilot study. CNS Spectr. 2007; 12:853–862. [PubMed: 17984858]

Song XW, Dong ZY, Long XY, Li SF, Zuo XN, Zhu CZ, He Y, Yan CG, Zang YF. REST: a toolkit for resting-state functional magnetic resonance imaging data processing. PloS one. 2011; 6:e25031. [PubMed: 21949842]

Staudinger MR, Erk S, Walter H. Dorsolateral prefrontal cortex modulates striatal reward encoding during reappraisal of reward anticipation. Cereb Cortex. 2011; 21:2578–2588. [PubMed: 21459835]

Stell BM, Brickley SG, Tang CY, Farrant M, Mody I. Neuroactive steroids reduce neuronal excitability by selectively enhancing tonic inhibition mediated by delta subunit-containing GABAA receptors. Proc Natl Acad Sci U S A. 2003; 100:14439–14444. [PubMed: 14623958]

Taylor A, Atkins R, Kumar R, Adams D, Glover V. A new Mother-to-Infant Bonding Scale: links with early maternal mood. Arch Womens Ment Health. 2005; 8:45–51. [PubMed: 15868385]

van Wingen G, van Broekhoven F, Verkes RJ, Petersson KM, Backstrom T, Buitelaar J, Fernandez G. How progesterone impairs memory for biologically salient stimuli in healthy young women. J Neurosci. 2007; 27:11416–11423. [PubMed: 17942736]

van Wingen GA, van Broekhoven F, Verkes RJ, Petersson KM, Backstrom T, Buitelaar JK, Fernandez G. Progesterone selectively increases amygdala reactivity in women. Mol Psychiatry. 2008; 13:325–333. [PubMed: 17579609]

Veer IM, Beckmann CF, Baerends E, Van Tol MJ, Ferrarini L, Milles J, Veltman DJ, Aleman A, Van Buchem MA, Van der Wee NJ, Rombouts SA. Reduced functional connectivity in major depression: A whole brain study of multiple resting-state networks. Neuroimage. 2009; 47

Vesga-Lopez O, Blanco C, Keyes K, Olfson M, Grant BF, Hasin DS. Psychiatric disorders in pregnant and postpartum women in the United States. Arch Gen Psychiatry. 2008; 65:805–815. [PubMed: 18606953]

Viguera AC, Tondo L, Koukopoulos AE, Reginaldi D, Lepri B, Baldessarini RJ. Episodes of Mood Disorders in 2,252 Pregnancies and Postpartum Periods. Am J Psychiatry. 2011

Weis S, Hausmann M, Stoffers B, Vohn R, Kellermann T, Sturm W. Estradiol modulates functional brain organization during the menstrual cycle: an analysis of interhemispheric inhibition. J Neurosci. 2008; 28:13401–13410. [PubMed: 19074013]

Yoo SS, Gujar N, Hu P, Jolesz FA, Walker MP. The human emotional brain without sleep--a prefrontal amygdala disconnect. Curr Biol. 2007; 17:R877–R878. [PubMed: 17956744]
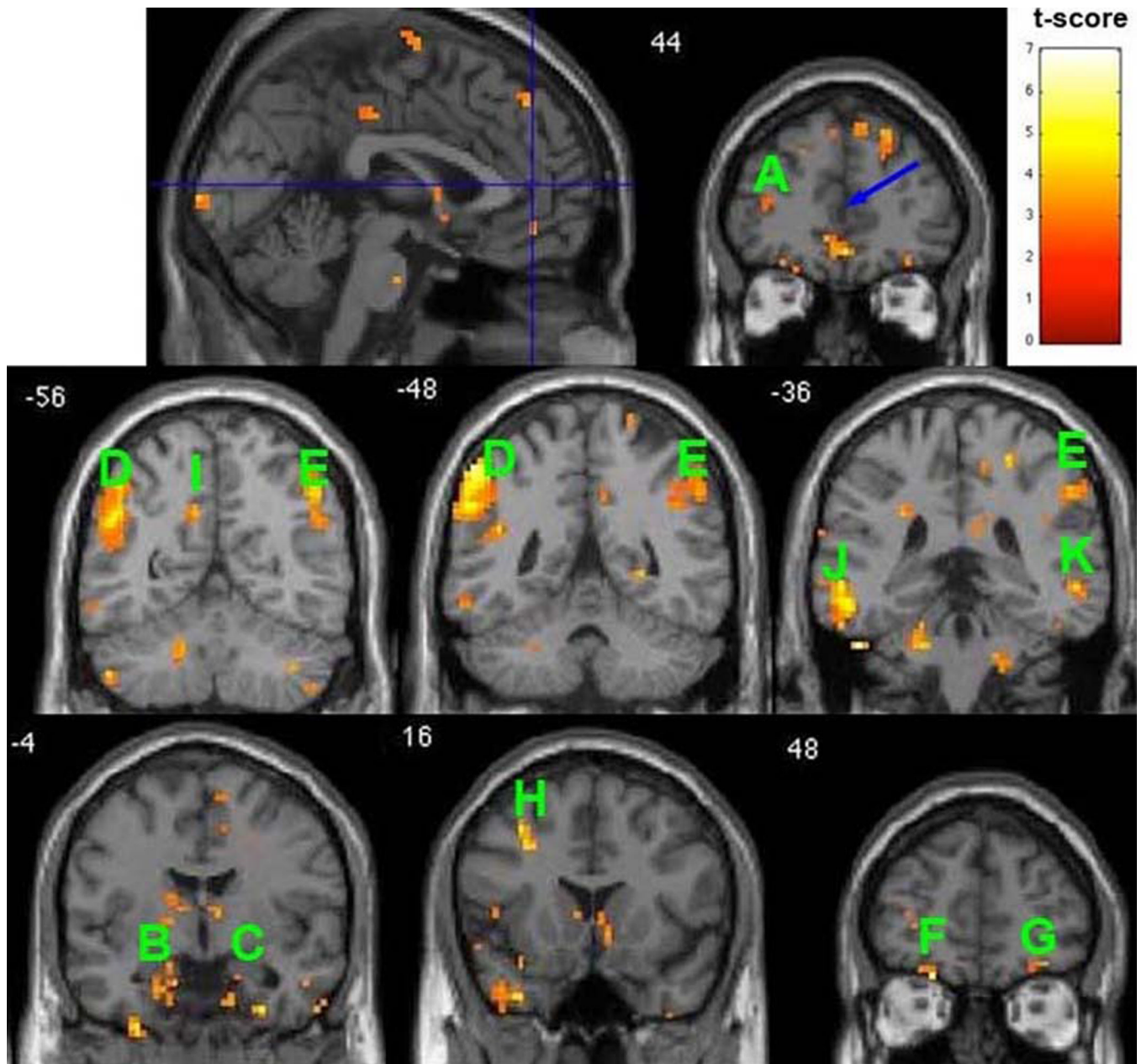
Figure 1.
Resting-state function connectivity maps with seed region (radius 5 mm) located at bilateral anterior cingulate cortices (ACC) (MNI coordinates: 0, 44, 10, indicated by the blue arrow) superimposed onto coronal sections. The map shows that healthy comparison subjects have significantly stronger connections with the seed region than those with postpartum depression (p<0.01, t-score>2.60, minimum of 5 voxels for each cluster, df=15). The approximate locations of selected clusters are labeled A–K. A: Left DLPFC, B: L AMYG, C: R AMYG, D: L Inferior Parietal Lobule, E: R Inferior Parietal Lobule, F: L Superior Frontal Gyrus, G: R Superior Frontal Gyrus, H: L Middle Frontal Gyrus, I: L Precuneus, J: L Middle Temporal Gyrus, K: R Middle Temporal Gyrus.
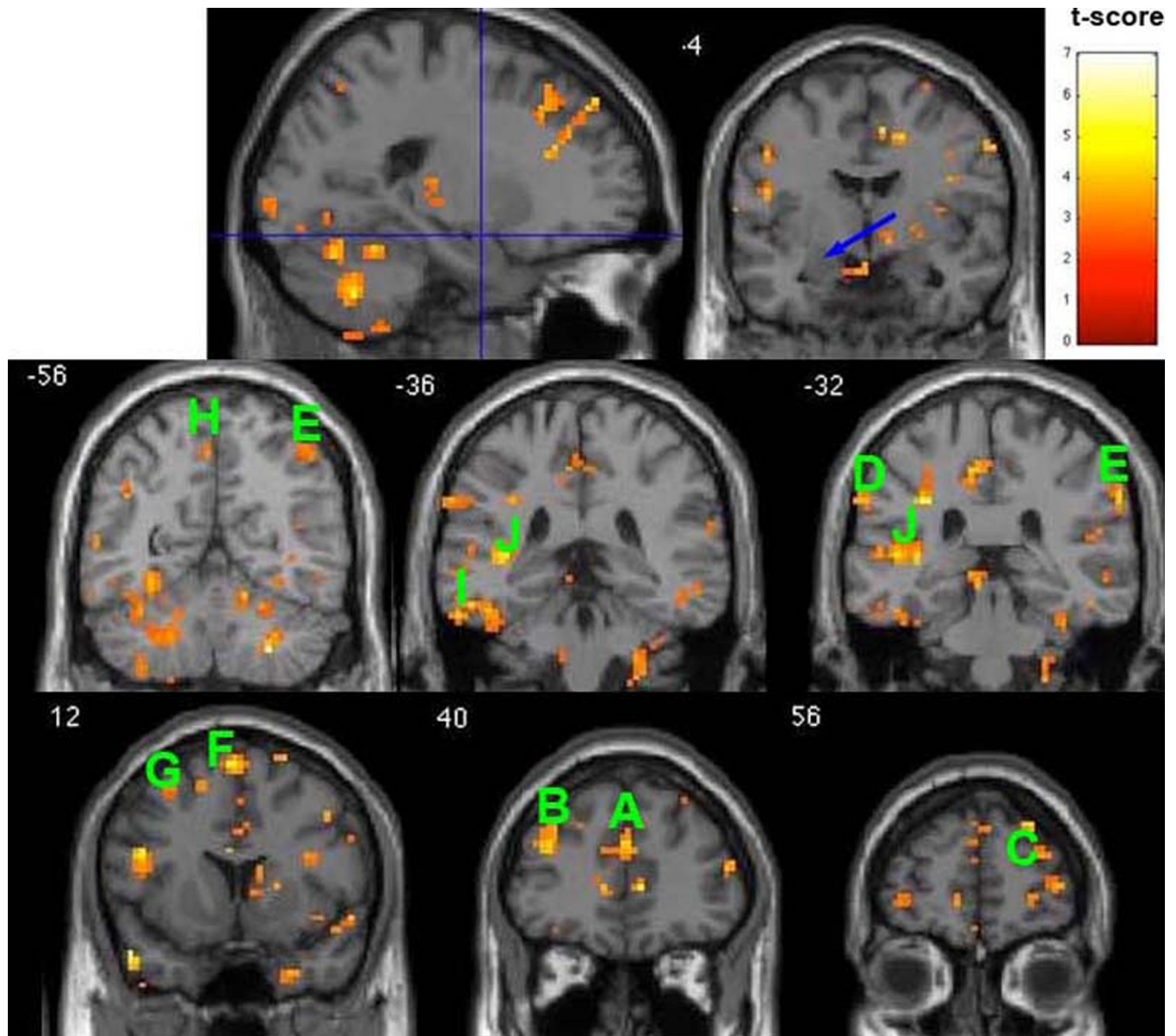
Figure 2.
Resting-state function connectivity maps with seed region (radius 5 mm) at left amygdala (AMYG) (MNI coordinates: −20, −3, −16, indicated by the blue arrow) superimposed onto coronal sections. The map shows areas that healthy comparison subjects have significantly stronger connections with the seed region than those with postpartum depression (p<0.01, t-score>2.60, minimum of 5 voxels for each cluster, df=15). The approximate locations of selected clusters are labeled A–J. A: ACC, B: L DLPFC, C: R DLPFC, D: L Inferior Parietal Lobule, E: R Inferior Parietal Lobule, F: L Superior Frontal Gyrus, G: L Middle Frontal Gyrus, H: L Precuneus, I: L Inferior Temporal Gyrus, J: L Superior Temporal Gyrus.
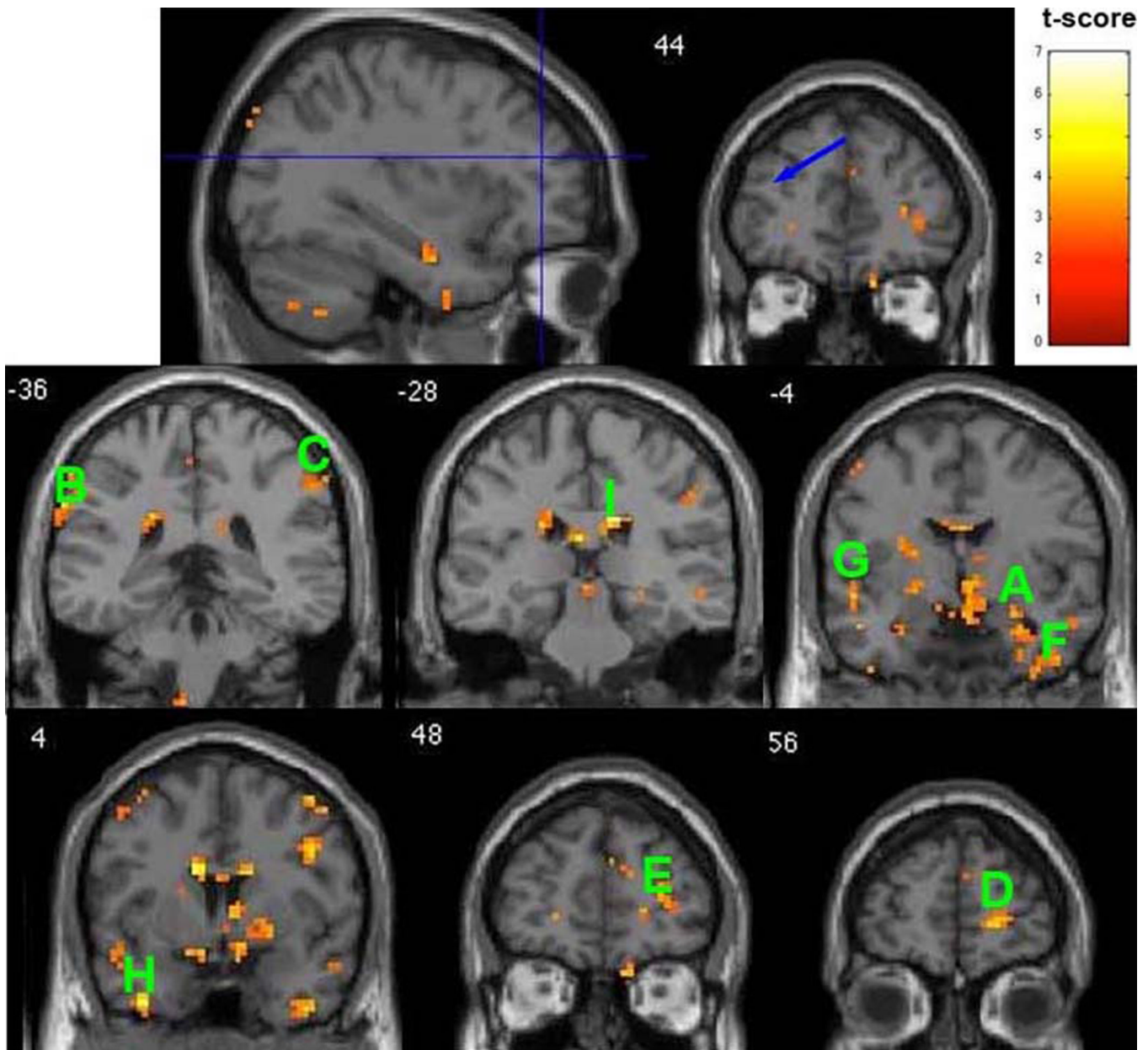
Figure 3.
Resting-state function connectivity maps with seed region (radius 7mm) located at left dorsolateral prefrontal cortex (DLPFC) (MNI coordinates: −34, 42, 20, indicated by the blue arrow) superimposed onto coronal sections. The map shows that healthy comparison subjects have significantly stronger connections than those with postpartum depression (p<0.01, t-score>2.60, minimum of 5 voxels for each cluster, df=15). The approximate locations of selected clusters are labeled A–I. A: right AMYG, B: L Inferior Parietal Lobule, C: R Inferior Parietal Lobule, D: R Superior Frontal Gyrus, E: R Middle Frontal Gyrus, F: R Inferior Temporal Gyrus, G: L Superior Temporal Gyrus, H: L Middle Temporal Gyrus, I: R Cingulate Gyrus.

TABLE 1

Demographic factors and assessments

	Healthy Control (HCS, n=9)			Postpartum Depressed (PPD, n=8)			p-value
	Mean	SD	Percent	Mean	SD	Percent	
Demographic Characteristics							
Age (years)	30.67	3.81		28.62	5.93		ns
Right-handed			87.5%			71.4%	ns
Smoker			0%			0%	ns
Primiparous			33.33%			25%	ns
Pre-term delivery (i.e. <37 weeks gestation)			0%			0%	ns
Labor and delivery							ns
• induced delivery			14.29%			37.5%	
• vaginal delivery			71.43%			87.5%	
• Cesarean section			28.57%			12.5%	
• neonatal intensive care unit admission			0%			0%	
Time since delivery (days)	57.44	10.2		47.75	14.26		ns
Breastfeeding(day of MRI)							ns
•full-time breastfeeding without formula supplementation			42.86%			42.86%	
• part-time breastfeeding with formula supplementation			28.57%			28.57%	
• formula feeding only			28.57%			28.57%	
Presence of menstrual spotting since delivery			28.57%			25%	ns
Diagnosis, Mood & Psychosocial Assessments							
History of major depressive episode			0%			87.5%	<0.001
History of postpartum depression			0%			25%	ns
Dysthymic disorder			0%			0%	ns
Generalized anxiety disorder			0%			50%	<0.05
Panic disorder without agoraphobia			0%			0%	ns
Panic disorder with agoraphobia			0%			12.5%	ns
Agoraphobia without panic disorder			0%			0%	ns
Social phobia			0%			37.5%	ns
Obsessive compulsive disorder			0%			25%	ns

	Healthy Control (HCS, n=9)			Postpartum Depressed (PPD, n=8)			p-value
	Mean	SD	Percent	Mean	SD	Percent	
Post-traumatic stress disorder			0%			12.5%	ns
History of substance abuse/dependence			0%			12.5%	ns
Eating disorder			0%			0%	ns
Current or past psychotic disorder, hypomanic or manic episode			0%			0%	ns
Edinburgh Postnatal Depression Scale	1.11	1.05		15.13	5.14		<0.001
Quick Inventory Depressive Symptoms	3.22	2.44		11.63	4.98		<0.005
Sheehan Patient Rated Anxiety Scale	3	2.92		35.62	23.36		<0.001
Sheehan Disability Scale-days unproductive	0	0		2.375	2.07		<0.01
Pittsburgh Sleep Quality Index	5.26	2.63		9.83	3.37		<0.05
Postpartum Social Support Questionnaire	10	7.38		34.33	35.61		ns
Mother-to-infant bonding scale	1.14	1.46		1.86	1.95		ns

Abbreviations: SD, standard deviation; ns, not significant; MRI, magnetic resonance imaging

TABLE 2

Regions where functional connectivity with the seed regions is significantly more for healthy postpartum subjects than subjects with unipolar postpartum (p<0.01, t-score>2.60, minimum of 5 voxels for each cluster, df=15)

Seed Area	Connected Location	Brodmann Area (BA)	peak MNI Coordinates x	y	z	Voxel Size	peak T-value
Anterior Cingulate Cortex (ACC)	L Inferior Parietal Lobule	BA40	-54	-48	48	168	6.00
	R Inferior Parietal Lobule	BA40	48	-57	42	130	4.37
	L Inferior Frontal Gyrus	BA45	-54	21	12	22	4.64
	R Inferior Frontal Gyrus	BA47	54	30	-6	5	3.61
	L Superior Frontal Gyrus	BA11	-21	48	-21	6	4.80
	L Superior Frontal Gyrus	BA10	-18	57	24	10	4.42
	L Superior Frontal Gyrus	BA6	-3	-6	72	12	3.56
	R Superior Frontal Gyrus	BA9	24	42	39	22	4.49
	L Middle Frontal Gyrus	BA8	-30	18	36	46	6.28
	L Middle Frontal Gyrus	BA11	-42	33	-12	4	5.36
	R Middle Frontal Gyrus	BA9	42	24	39	36	4.40
	R Medial Frontal Gyrus	BA11	3	45	-12	20	4.82
	R Medial Frontal Gyrus	BA6	9	-6	63	10	3.66
	R Postcentral Gyrus	BA3	24	-36	57	5	4.00
	L Precuneus	BA7	-9	-57	33	10	3.71
	R Middle Temporal Gyrus	BA21	57	-36	-6	24	4.51
	L Middle Temporal Gyrus	BA21	-56	-36	-12	12	2.61
	R Parahippocampal	N/A	21	-6	-21	24	2.78
	L Caudate	N/A	-6	6	0	56	5.35
	L Thalamus	N/A	-15	-21	9	8	4.00
	R Cerebellum Posterior Lobe	N/A	45	-54	-51	8	3.48
Left Amygdala (AMYG)	L Inferior Parietal Lobule	BA40	-63	-33	33	35	3.67
	R Inferior Parietal Lobule	BA42	63	-39	21	5	4.11
	R Superior Parietal Lobule	BA7	36	-63	51	9	3.87
	L Inferior Frontal Gyrus	BA47	-48	30	-9	6	3.51
	R Inferior Frontal Gyrus	BA9	54	21	24	12	4.75

Seed Area	Connected Location	Brodmann Area (BA)	peak MNI Coordinates			Voxel Size	peak T-value
			x	y	z		
	L Superior Frontal Gyrus	BA6	-3	12	66	56	4.89
	R Superior Frontal Lobe	BA10	27	54	0	13	4.84
	L Middle Frontal Gyrus	BA8	-51	9	45	9	3.37
	R Middle Frontal Gyrus	BA8	30	36	51	27	5.76
	L Medial Frontal Gyrus	BA10	-9	48	15	16	3.21
	R Medial Frontal Gyrus	BA10	3	51	6	8	3.35
	L Precentral Gyrus	BA3	-51	-18	36	14	4.27
	R Precentral Gyrus	BA6	63	-3	39	22	3.71
	R Postcentral Gyrus	BA40	57	-27	18	24	4.28
	L Precuneus	BA7	-3	-54	51	12	3.00
	R Precuneus	BA7	9	-39	48	11	3.61
	L Inferior Temporal Gyrus	BA20	-60	-36	-24	14	4.02
	L Superior Temporal Gyrus	BA41	-36	-36	6	44	5.50
	R Superior Temporal Gyrus	BA22	66	-12	3	14	3.91
	R Superior Temporal Gyrus	BA38	45	21	-24	9	3.67
	L Middle Temporal Lobe	BA22	-51	12	-27	26	5.29
	R Middle Temporal Gyrus	BA21	60	-42	-9	56	3.96
	R Inferior Occipital Gyrus	BA19	36	-72	-9	12	4.83
	R Lingual Gyrus	BA18	3	-84	-9	87	4.90
	L Fusiform Gyrus	BA20	-45	-36	-21	26	3.91
	R Fusiform Gyrus	BA19	33	-63	-12	14	4.46
	L Cerebellum Posterior Lobe	N/A	-21	-60	-42	211	5.14
	R Cerebellum Posterior Lobe	N/A	36	-39	-39	45	4.18
Right Amygdala (AMYG)	L Inferior Parietal Lobule	BA40	-54	-33	39	29	3.95
	R Inferior Parietal Lobule	BA40	51	-45	45	99	4.30
	L Inferior Frontal Gyrus	BA45	-42	21	3	25	4.34
	R Inferior Frontal Gyrus	BA9	63	9	30	13	4.57
	R Inferior Frontal Gyrus	BA46	51	42	12	14	3.67
	R Superior Frontal Lobe	BA9	12	18	66	5	3.98

Seed Area	Connected Location	Brodmann Area (BA)	peak MNI Coordinates			Voxel Size	peak T-value
			x	y	z		
	L Middle Frontal Gyrus	BA10	-33	39	33	13	4.13
	R Middle Frontal Gyrus	BA9	39	42	27	21	4.22
	L Medial Frontal Gyrus	BA10	-9	51	18	7	4.10
	L Medial Frontal Gyrus	BA6	-3	-15	72	7	3.52
	L Precentral Gyrus	BA6	-48	-3	27	36	4.33
	L Postcentral Gyrus	BA4	-51	-21	42	10	3.37
	R Postcentral Gyrus	BA4	27	-36	60	8	4.35
	L Precuneus	BA7	-12	-48	57	11	3.37
	L Superior Temporal Gyrus	BA38	-42	21	-30	11	3.74
	R Middle Temporal Gyrus	BA37	60	-66	6	8	3.92
	L Middle Temporal Gyrus	BA39	-57	-69	18	7	3.67
	L Caudate	N/A	-9	18	9	6	4.91
	R Caudate	N/A	12	15	12	6	3.12
	L Insula	BA13	-42	9	12	5	4.08
	R Supramarginal Gyrus	BA40	60	-60	30	11	3.40
	L Cingulate Gyrus	BA24	-15	-3	39	6	4.29
Left Hippocampus (HIPP)	L Inferior Parietal Lobule	BA39	-51	-45	45	70	5.42
	L Inferior Frontal Gyrus	BA44	-54	3	15	8	4.12
	R Superior Frontal Lobe	BA9	30	54	33	9	4.34
	R Middle Frontal Gyrus	BA9	45	30	42	47	5.16
	L Middle Frontal Gyrus	BA8	-33	21	33	21	4.38
	R Medial Frontal Gyrus	BA9	6	33	36	10	4.42
	L Precentral Gyrus	BA4	-15	-30	63	182	7.05
	L Precentral Gyrus	BA6	-39	-3	33	5	3.82
	R Postcentral Gyrus	BA5	42	-30	57	5	3.79
	R Postcentral Gyrus	BA40	51	-36	51	51	3.43
	L Precuneus	BA7	-9	-81	45	5	3.25
	R Precuneus	BA7	18	-66	42	26	3.07
	L Superior Temporal Gyrus	BA22	-60	-3	6	11	4.53

Seed Area	Connected Location	Brodmann Area (BA)	peak MNI Coordinates			Voxel Size	peak T-value
			x	y	z		
	L Superior Temporal Gyrus	BA38	−36	18	−36	5	4.2
	L Middle Temporal Gyrus	BA37	−63	−42	−18	10	3.65
	L Thalamus	N/A	−9	−9	0	6	4.42
	L Fusiform Gyrus	BA17	−27	−93	−24	12	4.00
	L Cingulate Gyrus	N/A	−3	−18	30	22	3.97
Right Hippocampus (HIPP)	L Inferior Parietal Lobule	BA40	−48	−48	21	8	5.38
	L Inferior Frontal Gyrus	BA46	−54	15	21	21	3.33
	R Inferior Frontal Gyrus	BA9	51	0	24	5	3.67
	L Superior Frontal Gyrus	BA9	−24	33	33	6	4.22
	R Superior Frontal Gyrus	BA10	30	66	−6	18	4.62
	R Superior Frontal Gyrus	BA6	6	9	60	27	4.16
	L Middle Frontal Gyrus	BA8	−27	24	33	7	3.36
	R Medial Frontal Gyrus	BA6	12	−3	63	29	4.18
	L Precentral Gyrus	BA6	−45	−6	42	13	3.63
	L Postcentral Gyrus	BA4	−39	−21	51	24	4.00
	R Precuneus	BA7	15	−66	33	9	3.34
	L Superior Temporal Gyrus	BA38	−51	3	−12	17	5.28
	R Superior Temporal Gyrus	BA22	54	−39	6	7	3.44
	L Middle Temporal Gyrus	BA38	−54	9	−33	23	4.68
	L Middle Temporal Gyrus	BA21	−66	−30	0	8	3.64
	R Caudate	N/A	9	9	9	16	4.10
	L Cingulate Gyrus	BA6	−9	−15	39	142	5.72
Left DorsoLateral PreFrontal Cortex (DLPFC)	L Inferior Parietal Lobule	BA40	−63	−39	33	13	4.39
	L Inferior Parietal Lobule	BA40	−54	−39	39	8	3.42
	R Inferior Parietal Lobule	BA40	57	−36	42	13	3.2
	R Inferior Frontal Gyrus	BA6	45	3	36	17	4.56
	R Superior Frontal Lobe	BA10	21	54	3	23	5.24
	R Middle Frontal Gyrus	BA10	30	48	12	14	3.66
	R Precentral Gyrus	BA11	51	0	54	1	3.6

Seed Area	Connected Location	Brodmann Area (BA)	peak MNI Coordinates			Voxel Size	peak T-value
			x	y	z		
	L Precentral Gyrus	BA6	-48	0	54	13	3.22
	R Postcentral Gyrus	BA3	66	-12	24	13	4.69
	R Inferior Temporal Gyrus	BA20	48	-3	-39	16	3.47
	L Superior Temporal Gyrus	BA21	-51	-3	-9	18	3.92
	R Superior Temporal Gyrus	BA38	39	18	-33	14	3.64
	L Middle Temporal Gyrus	BA21	-39	3	-39	14	5.43
	R Middle Temporal Gyrus	BA38	42	3	-42	14	4.82
	R Parahippocampal Gyrus	N/A	27	-3	-18	8	3.48
	L Parahippocampal Gyrus	N/A	-30	-9	-21	15	4.92
	R Caudate	N/A	-9	15	9	7	3.18
	R Cingulate Gyrus	N/A	15	-27	27	51	6.15
Right DorsoLateral PreFrontal Cortex (DLPFC)	L Inferior Parietal Lobule	BA40	-63	-39	27	84	4.99
	R Inferior Parietal Lobule	BA40	57	-36	45	36	5.31
	L Inferior Frontal Gyrus	BA6	-33	3	33	21	6.09
	L Superior Frontal Gyrus	BA6	-9	3	72	72	4.21
	R Superior Frontal Gyrus	BA6	21	-9	78	8	3.28
	L Middle Frontal Gyrus	BA6	-51	3	45	56	4.36
	R Middle Frontal Gyrus	BA10	45	45	-3	6	4.41
	L Precentral Gyrus	BA44	-54	9	12	26	5.39
	R Precentral Gyrus	BA44	48	6	9	9	3.95
	L Postcentral Gyrus	BA2	-57	-24	48	37	4.28
	R Postcentral Gyrus	BA2	51	-27	36	23	4.82
	R Inferior Temporal Gyrus	BA19	60	-57	-9	5	3.21
	R Inferior Temporal Gyrus	BA20	39	-3	-45	12	4.33
	L Superior Temporal Gyrus	BA22	-60	-30	6	6	3.83
	R Superior Temporal Gyrus	BA38	24	12	-39	12	3.07
	R Superior Temporal Gyrus	BA38	45	12	-30	13	3.95
	L Middle Temporal Gyrus	BA39	-48	-78	18	5	3.34
	L Middle Temporal Gyrus	BA21	-57	-3	-3	11	7.22

Seed Area	Connected Location	Brodmann Area (BA)	peak MNI Coordinates			Voxel Size	peak T-value
			x	y	z		
	L Middle Occipital Gyrus	BA39	−51	−81	6	19	4.4
	L Fusiform Gyrus	BA37	−48	−57	−21	10	4.04
	R Fusiform Gyrus	BA19	39	−63	−18	3	3.61
	L Thalamus	N/A	−15	−9	12	7	6.29
	L Insula	N/A	−36	−15	18	72	5.46
	L Insula	N/A	−30	18	9	11	3.42
	L Cingulate Gyrus	N/A	−12	3	27	9	4.54
	R Cingulate Gyrus	N/A	9	−15	27	29	3.86

Abbreviations: L, left; R, right; N/A, not applicable;

[†] ACC spherical seed centered at MNI coordinate (0,44,10) with a radius of 5mm (Blakemore, SJ, 2008; Chai, XJ et al., 2011b; Cullen, KR et al., 2009; Kelly, AM et al., 2009; Margulies, DS et al., 2007).

[*] Left (Conklin, SM et al., 2007; Ernst, M et al., 2005; Evans, KC et al., 2008; Gianaros, PJ et al., 2008; Shin, LM et al., 2005; Yoo, SS et al., 2007) and right AMYG (Ernst, M et al., 2005; Evans, KC et al., 2008; Gianaros, PJ et al., 2008; Shin, LM et al., 2005; Yoo, SS et al., 2007) spherical seed centered at MNI coordinate (−20, −3, −16) and (20, −3, −16) with a radius of 5mm, respectively.

[^] Left (Conklin, SM et al., 2007; Kahn, I et al., 2008; McClure, SM et al., 2004; Shin, LM et al., 2005) and right HIPP (Conklin, SM et al., 2007; Kahn, I et al., 2008; McClure, SM et al., 2004; Shin, LM et al., 2005) spherical seed centered at MNI coordinate (−25, −26, −10) and (25, −26, −10) with a radius of 5mm, respectively.

[#] Left (Hayama, HR&Rugg, MD, 2009; Qin, S et al., 2009; Silton, RL et al., 2010; Staudinger, MR et al., 2011) and right DLPFC (Hayama, HR&Rugg, MD, 2009; Qin, S et al., 2009; Silton, RL et al., 2010; Staudinger, MR et al., 2011) spherical seed centered at MNI coordinate (−34, 42, 20) and (34, 42, 20) with a radius of 7mm, respectively.

TABLE 3

Mean (+SD) Plasma GABAergic neuroactive steroid concentrations (ng/mL) in perinatal women as a function of postpartum depressed status

	Time Point[†]	Healthy Control			High-risk subjects who developed PPD			p-value
		N	Mean	SD	N	Mean	SD	
Progesterone	pregnancy	4	280.17	293.13	3	380.27	473.52	0.72
	postpartum	7	2.70	1.59	6	2.73	2.17	0.94
Allopregnanolone	pregnancy	4	16.25	6.72	3	26.69	4.54	0.08
	postpartum	7	0.36	0.12	5	0.30	0.08	0.37
Pregnenolone	pregnancy	4	7.34	2.64	3	7.02	2.08	1.0
	postpartum	8	1.93	1.06	7	1.34	0.61	0.30
Pregnanolone	pregnancy	4	13.10	9.24	3	11.99	7.29	1.0
	postpartum	8	0.55	0.22	7	0.42	0.31	0.42

Abbreviations: ng/mL, nanograms per milliliter; SD, standard deviation; ns: not significant at p>0.05.

[†]The pregnancy time point was between 34–36 weeks gestation and the postpartum time point was between 3–9 weeks for all subjects. Some blood samples in pregnancy were not available for analysis or in the postpartum had levels of quantification below detection, resulting in neuroactive steroid concentration data at both time points for most but not all subjects.

The limits of detection for each of the steroids were defined at 0.2 ng/mL.